JOURNAL OF
EMERGING INVESTIGATORS

Article

Fractal dimensions of crumpled paper

Curtis Zhou[1], Carey Witkov[2]
[1] The Peddie School, Hightstown, New Jersey
[2] Embry-Riddle Aeronautical University, Daytona Beach, Florida

SUMMARY

Fractals are infinitely complex shapes that can be split into two types: mathematical fractals and statistical fractals. Mathematical fractals are infinitely complex and self-similar across multiple scales, whereas statistical fractals are not self-similar but can be applied to real life. Crumpling paper is a mathematical fractal process whereby a sheet of paper undergoes deformation via compression. This yields a three-dimensional structure that introduces isotropic and homogenous spaces of varying sizes inside the crumpled paper structure. There is a hierarchy of spaces: a few large, a moderate number of medium, and many small. Consequently, a crumpled paper ball is a fractal object. Fractal dimension is a non-integer measure of an object's "roughness" and is useful in studying natural objects consisting of many irregular shapes like crumpled paper. In this study, we determined the fractal dimension of a sheet of paper crumpled into a series of spheres of decreasing radii using continuous X^2 analysis. The result is a tested model relating mass to radius via fractal dimension for crumpled paper, which in this study, yielded a fractal dimension of 2.40. Using Chi-Squared, we were able to test and validate our model and compare it to other experiments' results to verify consistency, offering advantages over more conventional least squares.

INTRODUCTION

Crumpling is a process whereby a piece of paper undergoes deformation to yield a three-dimensional structure with varying sizes of spaces inside the paper. The study of crumpling objects such as paper provides a useful mathematical model that can be used to describe or predict the behavior of other objects with fractal properties. Describing irregular curves and surfaces like crumpled paper has been a pivotal and significant topic in our understanding of science, at both a macroscopic and microscopic level, throughout the years, starting with attempts to measure the coastline of countries (1).

In 1975, Benoit Mandelbrot proposed fractal geometry to address the ambiguity caused by the absence of fitting geometric representations for irregular curves and non-smooth objects (2). Fractal dimension characterizes an object's dimension on a continuum, allowing non-integer values, making it suitable for measuring the "roughness" of an object (2). We are used to objects with integer dimensions; for example, a line is one-dimensional, a plane is two-dimensional, and a sphere is three-dimensional. These integer dimensions apply to ideal shapes. However, when we look at natural shapes like crumpled paper that have a range of spaces with varying sizes inside of them, it raises the question of whether the shape is three-dimensional, two-dimensional, or something in-between. Fractal dimensions help resolve this problem. Fractal dimensions can vary between one and two for a curve, or between two and three for a surface (depending on the compressibility of the materials). As a simple, single number to characterize a curve or surface, fractal dimensions have wide appeal and have been applied in biology, aerodynamics, statistical physics, chaos theory, and more (3)(4)(5).

There is a well-known power law scaling relationship between mass and radius for a sphere:

$$m = \rho R^3 \tag{1}$$

Frame proposes a model for the relation between mass and radius based on fractal dimension (6). The cubic dependence of mass on radius (or side) is independent of the shape. In addition, any deviations from sphericity are accounted for by averaging over the measurements from each axis. If we allow the exponent to be a variable, we can identify fractal dimension as the exponent (n) of radius, where n = 2 or a two-dimensional object and n = 3 for a three-dimensional object. Hence, we have:

$$m = \rho R^n \tag{2}$$

where m is mass, R is the radius, ρ is the fractal density, and n is the fractal dimension. Next, we propose a linear model. Taking logs of both sides, we obtain:

$$n \log R = \log m - \log \rho \tag{3}$$

which can be rearranged as a two-parameter linear model, y = mx + b:

$$\log R = \frac{1}{n}\log m - \frac{1}{n}\log \rho \tag{4}$$

From this two-parameter linear model (Eq. 4), we can determine the fractal dimension as the reciprocal of the best-fit slope to the results of the experiment. While the mass of crumpled paper is a function of radius, the model is expressed as radius as a function of mass (logR and logm). The reason is, in this investigation, mass is the independent variable and radius is the dependent variable. While a one-parameter (slope only) model that neglects density is sufficient for calculating fractal dimension, the more physically realistic two-parameter (slope and intercept) model that includes density is used.

In this investigation, we calculated the fractal dimension of crumpled paper as the slope of a linear model obtained using chi-squared minimization and implemented in a Python script. We took measurements on samples of paper crumpled into spheres and hypothesized that the fractal dimension of crumpled paper would be found within the range of two to three. We predicted this outcome because the range of spaces with varying sizes inside the crumpled paper ball reduces its dimensionality. We found that the fractal dimension of crumpled paper was between two and three, which supported our hypothesis. Understanding the geometry of crumpling is relevant on many levels. Modeling this process allows us to predict many processes and develop cutting-edge tools, such as developing cost-effective biomarkers from EEG (electroencephalogram) readings. By using fractal dimension to analyze EEG time series, we can examine atypical temporal-scale-specific fractal changes that lead to cognitive decline, such as Alzheimer's Disease (7). We can also enhance the microscopic crimping of graphene membranes used in high-performance batteries and supercapacitors (8).

RESULTS

Data for our analysis consisted of 37 photographs taken from our own experiment. We cut identical sheets of A4 paper into different sizes (1/8th sheet of paper, 1/4 sheet of paper, 1/2 sheet of paper, and one whole sheet of paper), then we crumpled the sheets of paper into paper balls **(Figure 1)**. We were also able to use this principle to estimate the masses of the variously sized crumpled paper relative to the mass of one A4 sheet of paper, computing the mass of the crumpled paper balls on a basis of 1 sheet of paper, 1/2 sheet of paper, 1/4 sheet of paper, and 1/8 sheet of paper. This technique avoided the need for mass measurements that would exceed the measurement resolution of available balances for small-radius crumpled paper balls. Further, this technique was consistent with our Chi-squared approach, which assumed that all variability is in the dependent variable (radius) and not the independent variable (mass). To increase the accuracy of our experiment, we took three perspectives of each crumpled paper ball: a top view, a frontal side view, and a rear side view **(Figure 2)**.

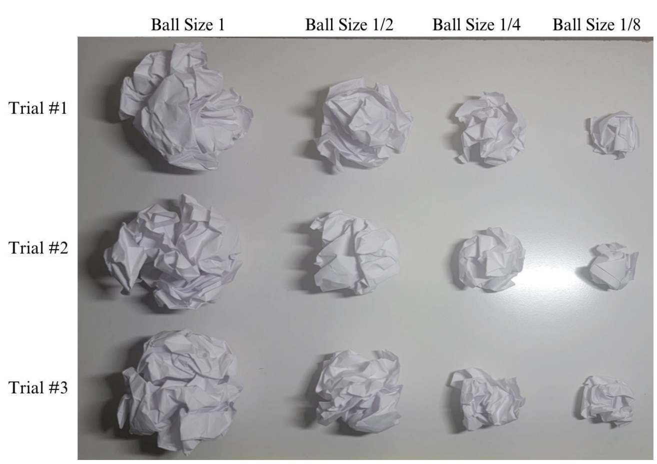

Figure 1: Crumpled paper used in the experiment. All crumpled paper balls and relative sizes (per fraction of one whole A4 sheet of paper) used in experimental trials #1-3: ball size 1, ball size 1/2, ball size 1/4, and ball size 1/8.

We used the software package GeoGebra (9) to precisely measure crumpled paper diameters (using relative units) and then convert those measurements to radii to fit our model. We made three random measurements of each crumpled ball photographic image. We repeated each measurement for all three perspectives, all sizes of crumpled paper ball, and all three crumpled paper balls. We took the average of these measurements and used them in our model **(Table 1)**. Since fractal dimension is unitless as the slope of log(m) versus log(R), the use of relative units is actually preferred. Note that although the model refers to the radius and the measurements were made on the diameter, it is not important to the result as the figures were converted for the fitting.

We then inserted the data into a Python script and ran it in Google Colaboratory (10, 11). This script provided a best-fit estimate of the fractal dimension and a X^2_{min} good-fit range (GFR) that was used to test the model. The GFR can be calculated as (12):

$$-GFR = N - \sqrt{2N} \ and \ +GFR = N \pm \sqrt{2N} \tag{5}$$

where N is the number of data points, i.e., the number of mean values, which for our experiment is $N = 4$. Therefore the X^2_{min} GFR for our experiment is [1.17, 6.83]. We inputted the mass and diameter values by taking logarithms of diameter and mass, while we took the A_{best} and B_{best} values based on a scope of 10% outside of the obtained values, allowing us to see the contours of the graph better. Testing whether X^2_{min} lies within the GFR is the method of model testing used in this analysis **(Figure 3)**.

We utilized a Chi-squared analysis, following the approach used by Witkov and Zengel (12). Chi-squared is defined as:

$$\chi^2 = \sum \frac{\left(y_i - y_{model_i}\right)^2}{\sigma_i^2} \tag{6}$$

Minimizing Chi-squared is a weighted least squares method in which the contribution of each data point to the curve fit is inversely weighted by the data point's uncertainty (i.e., standard error σ). In the one-parameter model (Y = Ax), chi-squared is a parabola, but in the two-parameter model (Y = Ax + B), Chi-squared is a paraboloid. Hence, the minimum value of chi-squared (X^2_{min}) is the minimum of the paraboloid and occurs at the point in the parameter plane given by (A_{best}, B_{best}), thus yielding the best-fit values for parameters A and B. To determine the contours of the paraboloid needed to find the values of Chi-squared that enclose 68% and 95% of the total probability: X^2_{268} and X^2_{295} we can write the integral of a probability density function p(x) up to the value of x which is called the cumulative distribution function c(x):

$$c(x) = \int_0^{\chi^2{}_{68}} p(\chi^2)d(\chi^2) = \int_0^{\chi^2{}_{68}} \frac{1}{2}e^{-\chi^2/2}d(\chi^2) \tag{7}$$

Setting c(X^2) = 0.68, we foud X^2_{268} = 2.3. Similarly, setting c(X^2) = 0.95, we found X^2_{95} = 6. With this, we built our contour lines with X^2_{min} + 2.3 and X^2_{min} + 6 These contours were displayed in a plot and were helpful when a parameter reference value was known (Figure 3B). If the reference value lies outside the 2σ contour, the model should be rejected. For the fractal dimension of crumpled paper, reference parameter values were not available, so chi-squared model testing was based on whether X^2_{min} is within the GFR.

From our results, we obtained a best-fit data plot and a

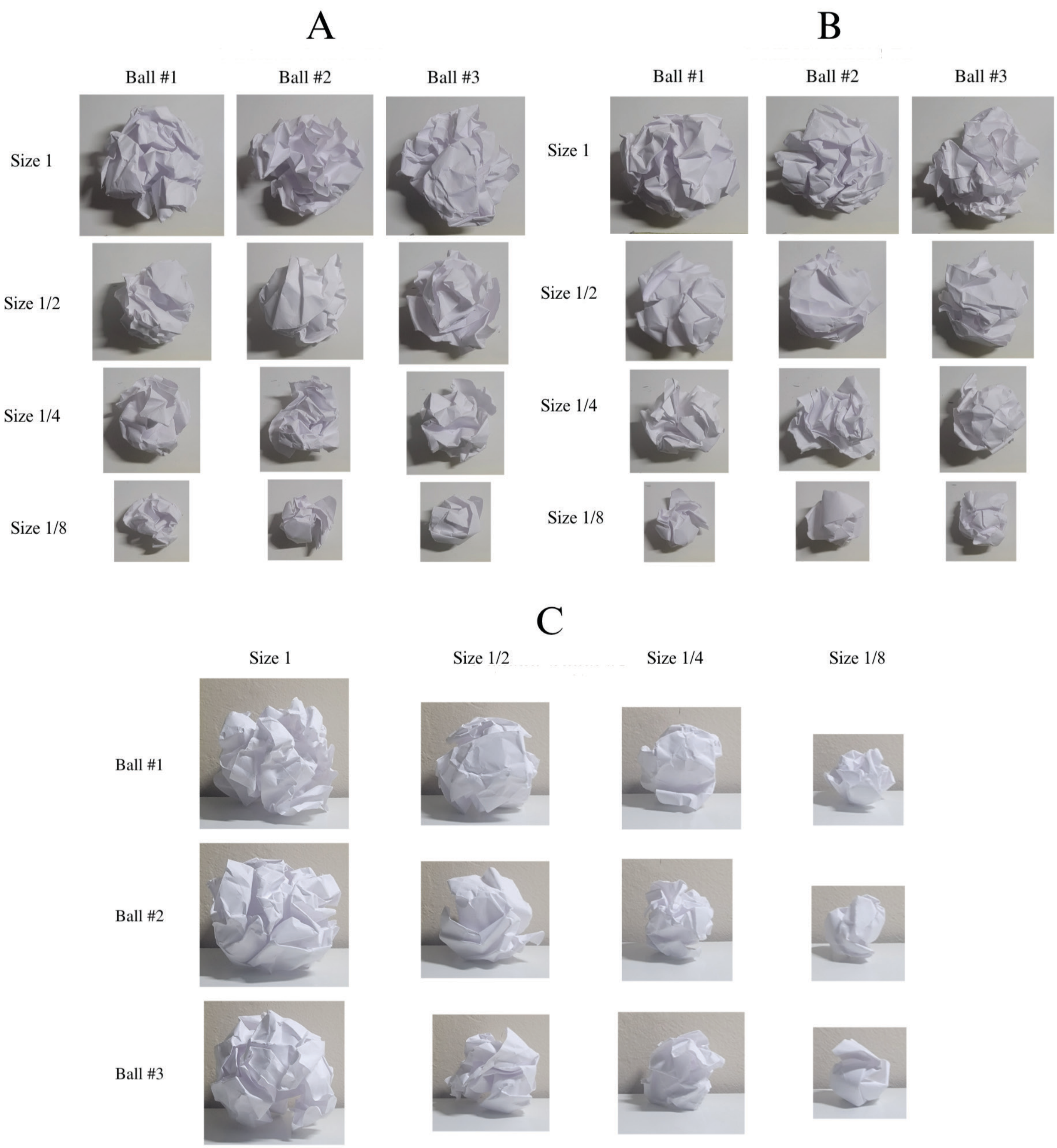

Figure 2: Perspectives of crumpled paper taken for measurements. All crumpled balls and relative sizes (per fraction of one whole A4 sheet of paper) with top view (a), bottom view (b), and side view (c) visual perspectives: ball size 1, ball size 1/2, ball size 1/4, and ball size 1/8.

plot of chi-squared contours **(Figure 3)**. The fractal dimension estimated (n = $1/A_{best}$) obtained for the crumpled paper balls was 2.40. The corresponding X^2_{min} value obtained was 3.35, within the X^2_{min} GFR for N = 4, which is [1.17, 6.83]. Therefore, the particular two-parameter linear model obtained should not be rejected.

DISCUSSION

In a three-dimensional space, a fractal dimension of two would represent a flat circle, while a fractal dimension of three would represent a sphere. Our results showed that the fractal dimension of the crumpled paper was between dimension n = 2 and n = 3. We expected this result as the crumpled paper ball presented itself as a three-dimensional form but never truly attained this status due to the amount of space present inside it. Our experimental results leaned slightly towards dimension n = 2 than n = 3, likely due to the type of paper used to create the crumpled paper balls. This suggested that the crumpled paper balls were made of relatively rigid sheets of paper as the fractal dimension fell near 2 for our results. This is because rigid paper increases the amount of space in the crumpled paper ball, allowing it to

	Top View	Side View (Front)	Side View (Back)	$SE_{Diamter}$
Ball Mass 1 (Avg)	6.90	7.00	6.20	0.032
Ball Mass 1/2 (Avg)	4.20	5.20	4.70	0.053
Ball Mass 1/4 (Avg)	3.80	3.60	3.40	0.027
Ball Mass 1/8 (Avg)	3.00	2.50	2.60	0.048

Table 1: Quantitative data (relative units) for the experiment. We additionally calculated standard error for diameter measurements ($SE_{Diameter}$) values for each type of crumpled paper ball measured in the experiment.

appear more like a plane than a sphere, whereas softer paper decreases the space in the ball, allowing it to fill more of the three-dimensional space in which it is embedded (13).

The most prevalent difference between the method used to test the model in this experiment compared to that of other research lies in the use of Chi-squared itself. Compared to ordinary least squares, Chi-squared provides uncertainty for A_{best} and B_{best} values and gave us the ability to test and compare our models. The generation of the contour plot provides a good example of the benefits of this method **(Figure 3B)**. Not only did the contour plot provide us with a means to test our model, but it also provided the A_{best} and B_{best} values on the plot surrounded by 68% and 95% contour lines. This allowed us to compare our results with other experiments' results to verify consistency.

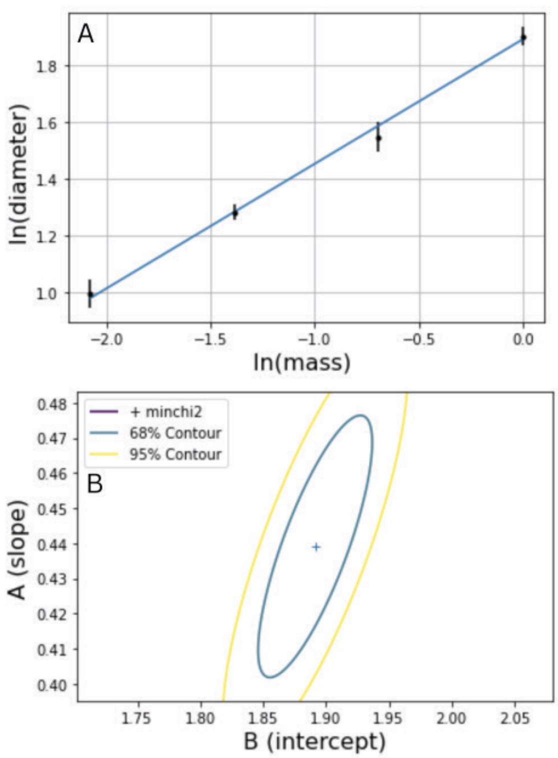

Figure 3: Best fit data (a) and chi-squared contours (b) plots attained from script. a) The graph of the ln(m) against the ln(R) values (relative units) for each of the balls analyzed.). Error bars depict standard error (n = 3). b) The graph of X^2_{min} in AB parameter plane with 68% and 95% contours. Statistical analysis performed by a chi-squared curve-fitting Python script that also performed the chi-squared analysis (n = 3).

Inaccuracies in measurement of the crumpled paper ball diameters may have been one source of error. Error in the measurement for the radius of the smaller ball (Ball Mass 1/8) is larger than the error for the radii of the other balls **(Figure 3A)**. This is likely due to a measurement error using GeoGebra caused by zooming in and out on images, as zooming in on smaller ones created a greater percentage error for each measurement (9). Also, the different sizes of images taken **(Figure 2)** may have led to an error in measurement and formatting. The deviation from sphericity for the crumpled paper balls may have been another source of error. However, this source of error is averaged out by multiple measurements of each view and by averaging multiple views.

Applications of fractals and fractal dimensions exist in many fields, including biology for measuring dimensional properties of biological structures (3). Many objects in nature are composed of complex shapes that are not well-defined by simple Euclidean geometrical shapes. For example, fractal dimension can characterize lung structure, which can be approximated as a fractal set (14). Studies have also shown that fractals can be useful for yielding insights into the mechanisms of tumor growth and angiogenesis and for describing the pathological architecture of tumors (15).

Engineering applications of fractals and fractal dimensions exist in aerodynamics, where their geometrical properties can be used to reduce aerodynamic drag, and in the study of turbulence, which exhibits fractal properties (4). As mathematical fractals are infinitely complex and self-similar across many different scales, they can represent many dynamical systems. Future potential areas of research include looking into the mechanisms of tumor growth and reducing aerodynamic drag on vehicles.

MATERIALS AND METHODS

At the beginning of our experiment, a model was developed to describe the fractal dimension of crumpled paper (n). Our mathematical model was:

$$n \log R = \log m - \log \rho \quad (8)$$

which was rearranged to form a two-parameter linear model, y = mx + b:

$$\log R = \frac{1}{n}\log m - \frac{1}{n}\log \rho \quad (9)$$

Identical sheets of A4 paper were crumpled into paper balls in our experiment (16). To increase the accuracy of our experiment, we took three perspectives of each crumpled paper ball: a top view, a fontal side view, and a rear side view. To obtain the diameters of the crumpled paper balls that were later converted into radii, we uploaded the images into the software package GeoGebra (9) and used its measure tool to obtain precise results for our diameters. The variables for this experiment were the masses of the crumpled paper balls, and the radii of the crumpled paper balls.

Data was read by a Chi-squared curve-fitting Python script that also performed the Chi-squared analysis (12). The script provided the fractal dimension as the best-fit slope and tested goodness of fit. Values obtained included: A_{best}, B_{best}, the fractal dimension, X^2_{min}, N (number of data points), and the X^2_{min} GFR.

Received: December 2, 2021
Accepted: March 9, 2023
Published: August 10, 2023

REFERENCES

1. Mandelbrot, Benoit B. “Stochastic Models for the Earth's Relief, the Shape and the Fractal Dimension of the Coastlines, and the Number-Area Rule for Islands.” *PNAS,* National Academy of Sciences, 1 Oct. 1975, https://doi.org/10.1073/pnas.72.10.3825
2. Losa, Gabriele A, *et al.* “From Fractal Geometry to Fractal Analysis.” *Richardson, L.F. (1961) the Problem of Contiguity an Appendix to Statistics of Deadly Quarrels. General System Yearbook,* 6, 139-187. - References - Scientific Research Publishing, Applied Mathematics, Vol.7 No.4, 10 Mar. 2016, https://doi.org/10.4236/am.2016.74032 .
3. S.V., Buldyrev. “Fractals in Biology.” *Fractals in Biology,* Springer, New York, NY, 2009, https://doi.org/10.1007/978-0-387-30440-3_222.
4. Nedić, J, *et al.* “Drag and near Wake Characteristics of Flat ... - Iopscience.iop.org” *Drag and near Wake Characteristics of Flat Plates Normal to the Flow with Fractal Edge Geometries,* Iopscience, 14 Aug. 2013, https://doi.org/10.1088/0169-5983/45/6/061406.
5. Harris, William. “How Chaos Theory Works.” HowStuffWorks Science, *HowStuffWorks,* 23 Aug. 2020, science.howstuffworks.com/math-concepts/chaos-theory6.htm.
6. Frame, Michael. “Crumpled Paper Lab.” *Fractal Geometry,* Yale University, 2012, users.math.yale.edu/public_html/People/frame/Fractals/Labs/CrumpledPaperLab/CrumpledPaperLab.html.
7. Nobukawa, Sou, *et al.* “Atypical Temporal-Scale-Specific Fractal Changes in Alzheimer’s Disease EEG and Their Relevance to Cognitive Decline.” *Cognitive Neurodynamics,* vol. 13, no. 1, 2018, pp. 1–11, https://doi.org/10.1007/s11571-018-9509-x.
8. Cranford, Steven W., and Markus J. Buehler. “Packing Efficiency and Accessible Surface Area of Crumpled Graphene.” *Physical Review B,* vol. 84, no. 20, 2011, https://doi.org/10.1103/physrevb.84.205451.
9. GeoGebra. “App Downloads.” *GeoGebra App,* GeoGebra, 2021, www.geogebra.org/download.
10. Witkov, Carey. “Witkov/fractals_resources.” GitHub, GitHub, 26 Oct. 2020, github.com/witkov/fractals_resources.
11. Google. “Google Colaboratory.” *Google Colab,* Google, 2021, colab.research.google.com/notebooks/intro.ipynb.
12. Witkov, Carey, and Keith Zengel. *Chi-Squared Data Analysis and Model Testing for Beginners.* Oxford University Press, 2019.
13. Balankin, Alexander S., and Orlando Susarrey Huerta. “Entropic Rigidity of a Crumpling Network in a Randomly Folded Thin Sheet.” *Physical Review E,* vol. 77, no. 5, 2008, https://doi.org/10.1103/physreve.77.051124.
14. Lennon, Frances E., *et al.* “Lung Cancer—a Fractal Viewpoint.” *Nature Reviews Clinical Oncology,* vol. 12, no. 11, 2015, pp. 664–675, https://doi.org/10.1038/nrclinonc.2015.108.
15. Baish, James W., and Rakesh K. Jain. “Fractals and Cancer.” *Cancer Research, American Association for Cancer Research,* 15 July 2000, cancerres.aacrjournals.org/content/60/14/3683.
16. Gomes, M. A. F. “Fractal Geometry in Crumpled Paper Balls.” American Association of Physics Teachers, American Association of Physics TeachersAAPT, 1 July 1987, https://doi.org/10.1119/1.15094.